Physics Letters B 295 (1992) 159–168
North-Holland

PHYSICS LETTERS B

Proton and deuteron F_2 structure functions in deep inelastic muon scattering

New Muon Collaboration

Bielefeld University, CERN, Freiburg University, Max Planck Institut für Kernphysik, Heidelberg, Heidelberg University, Mainz University, Mons University, Neuchatel University, NIKHEF-K, Oxford University, Saclay DAPNIA/SPP, University of California, Santa Cruz, Paul Scherrer Institute, Torino University and INFN Torino, Uppsala University, Institute for Nuclear Studies, Warsaw, Warsaw University, Wuppertal University

P. Amaudruz [a,1], M. Arneodo [b], A. Arvidson [c], B. Badelek [d], G. Baum [e], J. Beaufays [f,2], I.G. Bird [g,3], M. Botje [a,4], C. Broggini [h,5], W. Brückner [g], A. Brüll [i], W.J. Burger [a,6], J. Ciborowski [f,7], R. van Dantzig [f], H. Döbbeling [g,8], J. Domingo [a,9], J. Drinkard [j], D. Dyring [c], H. Engelien [i], M.I. Ferrero [b], L. Fluri [h], P. Grafström [c,10], T. Granier [k], D. von Harrach [g,11], M. van der Heijden [f,4], C. Heusch [j], Q. Ingram [a], K. Janson-Prytz [c], M. de Jong [f,11], E.M. Kabuß [g,11], R. Kaiser [i], T.J. Ketel [f], F. Klein [ℓ], B. Korzen [m], U. Kruner [m], S. Kullander [c], K. Kurek [d], U. Landgraf [i], F. Lettenström [i], T. Lindqvist [c], G.K. Mallot [n,ℓ], C. Mariotti [b,12], G. van Middelkoop [n,f], A. Milsztajn [k], Y. Mizuno [g,13], J. Nassalski [o], D. Nowotny [g,14], J. Oberski [f], N. Pavel [m,15], C. Peroni [b], H. Peschel [m,16], B. Povh [g,p], R. Rieger [ℓ], K. Rith [g], K. Röhrich [ℓ,17], E. Rondio [d], L. Ropelewski [d], A. Sandacz [o], C. Scholz [g], R. Schumacher [a,18], U. Sennhauser [a,19], F. Sever [e,20], T.-A. Shibata [p], M. Siebler [e], A. Simon [g], A. Staiano [b], G. Taylor [q,21], M. Treichel [g,22], M. Virchaux [k], J.L. Vuilleumier [h], T. Walcher [ℓ], R. Windmolders [r] and F. Zetsche [g]

[a] *Paul Scherrer Institute, CH-5234 Villigen, Switzerland*
[b] *Istituto di Fisica, Universitá di Torino, I-10125 Turin, Italy*
[c] *Department of Radiation Science, University of Uppsala, S-75121 Uppsala, Sweden*
[d] *University of Warsaw, PL-00681 Warsaw, Poland*
[e] *Physics Department, Bielefeld University, W-4800 Bielefeld, FRG* [23]
[f] *NIKHEF-K, P.O. Box 4395, NL-1009 AJ Amsterdam, The Netherlands* [24]
[g] *Max Planck Institut für Kernphysik, W-6900 Heidelberg, FRG* [23]
[h] *Université de Neuchâtel, CH-2000 Neuchâtel, Switzerland*
[i] *Physics Department, Freiburg University, W-7800 Freiburg, FRG* [23]
[j] *Institute for Particle Physics, University of California, Santa Cruz, CA 95064, USA*
[k] *DAPNIA/SPP, CE Saclay, F-91191 Gif-sur-Yvette, France*
[ℓ] *Institut für Kernphysik, Mainz University, W-6500 Mainz, FRG* [23]
[m] *Physics Department, Wuppertal University, W-5600 Wuppertal, FRG* [23]
[n] *CERN, CH-1211 Geneva 23, Switzerland*
[o] *Institute for Nuclear Studies, PL-00681 Warsaw, Poland*
[p] *Heidelberg University, W-6900 Heidelberg, FRG* [23]
[q] *Nuclear Physics Laboratory, University of Oxford, Oxford OX1 3RH, UK*
[r] *Faculté des Sciences, Université de Mons, B-7000 Mons, Belgium*

Received 29 July 1992

The structure functions F_2^p and F_2^d measured by deep inelastic muon scattering at incident energies of 90 and 280 GeV are presented. These measurements cover a large kinematic range, $0.006 \leqslant x \leqslant 0.6$ and $0.5 \leqslant Q^2 \leqslant 55\ \mathrm{GeV}^2$, and include the first precise data at small x, where large scaling violations are observed. The data agree with earlier results from SLAC and BCDMS but exhibit differences with respect to those of EMC-NA2. Extrapolations to small x of recent phenomenological parton distributions are shown to disagree with the present results.

1. Introduction

The nucleon structure function $F_2(x, Q^2)$ reflects the momentum distribution of quarks in the nucleon, an important aspect of its internal structure. The Q^2 dependence of F_2 can be used to determine the scale parameter of QCD and the momentum distribution of the gluons. In addition, the value of F_2 at low x determines the reaction rates to be expected at very high energy colliders such as LHC and SSC. Knowledge of the structure function of the proton (F_2^p), and the deuteron (F_2^d) has steadily improved in recent years, due to deep inelastic electron and muon scattering experiments [1–5], but significant discrepancies between some of these results remain. In this letter we present new precise results for the structure functions, F_2^p and F_2^d, measured in a deep inelastic muon scattering experiment.

In the deep inelastic scattering of a muon from a nucleon, the differential cross section for one-photon exchange can be written in terms of the nucleon structure function, $F_2(x, Q^2)$, and the ratio of longitudinally to transversely polarised virtual photon absorption cross section, $R(x, Q^2)$, as

$$\frac{\mathrm{d}^2\sigma(x, Q^2)}{\mathrm{d}x\,\mathrm{d}Q^2} = \frac{4\pi\alpha^2}{Q^2}\frac{F_2(x, Q^2)}{x} \times \left(1 - y - \frac{Q^2}{4E^2} + \frac{y^2 + Q^2/E^2}{2[1 + R(x, Q^2)]}\right), \quad (1)$$

where $-Q^2$ is the four-momentum transfer squared and E is the energy of the incident muon. The two scaling variables x and y are defined as $x = Q^2/2M\nu$ and $y = \nu/E$, where ν is the energy of the virtual photon and M the proton mass.

2. The experiment

This experiment (NMC-NA37) was performed at the M2 muon beam line of the CERN SPS. The data presented here were taken during 1986 and 1987 at nominal incident muon energies of 90 and 280 GeV.

[1] Present address: TRIUMF, Vancouver, Canada, BC V6T 2A3.
[2] Present address: Trasys, Brussels, Belgium.
[3] Present address: DAPNIA, Saclay, F-91191 Gif-sur-Yvette, France.
[4] Present address: NIKHEF-H, NL-1009 AJ Amsterdam, The Netherlands.
[5] Present address: INFN, Laboratori Nazionali del Gran Sasso, I-67010 Assergi, Italy.
[6] Present address: Université de Genève, CH-1211 Geneva 4, Switzerland.
[7] Present address: University of Warsaw, PL-00681 Warsaw, Poland.
[8] Present address: GSI, W-6100 Darmstadt, FRG.
[9] Present address: CEBAF, Newport News, VA 23606, USA.
[10] Present address: CERN, CH-1211 Geneva 23, Switzerland.
[11] Present address: University of Mainz, W-6500 Mainz, FRG.
[12] Present address: INFN-Istituto Superiore di Sanita, I-00161 Rome, Italy.
[13] Present address: Osaka University, 567 Osaka, Japan.
[14] Present address: SAP AG,W-6909 Walldorf, FRG.
[15] Present address: DESY, W-2000 Hamburg 52, FRG.
[16] Present address: Gruner und Jahr AG & CoKG, W-2210 Itzhoe, FRG.
[17] Present address: IKP2-KFA, W-5170 Jülich, FRG.
[18] Present address: Carnegie Mellon University, Pittsburgh, PA 15213, USA.
[19] Present address: EMPA, W-8600 Dübendorf, Switzerland.
[20] On leave from Jozef Stefan Institut, Ljubljana, Yugoslavia; present address: NIKHEF-K, NL-1009 AJ Amsterdam, The Netherlands.
[21] Present address: University of Melbourne, Parkville, Victoria, Australia.
[22] Present address: Université de Neuchâtel, CH-2000 Neuchâtel, Switzerland.
[23] Supported by Bundesministerium für Forschung und Technologie.
[24] Supported in part by FOM, Vrije Universiteit Amsterdam and NWO.

The spectrometer was an upgraded version of the EMC apparatus [6,7]. Improvements relevant to this analysis are described below; further details can be found in refs. [8,9].

The proton and deuteron structure functions were measured simultaneously using two similar pairs of 3 m long targets exposed alternately to the beam. In one pair the upstream target was liquid hydrogen and the downstream target liquid deuterium, while in the other pair the order was reversed. The acceptance of the spectrometer was significantly different for the upstream and downstream targets, giving two separate determinations of the structure function for each material. The simultaneity of the measurements greatly reduced the uncertainty of the relative normalisation between the proton and deuteron structure functions.

The integrated incident muon flux was measured by two different methods. In addition to the method of the EM Collab. [10] which used a random trigger to sample the beam, a new trigger was installed. The total numbers of counts in two planes of the scintillator hodoscopes used to determine incident beam tracks were recorded, and prescaled to form this trigger. In both methods the beam tracks present in the triggers were reconstructed off line, in the same way as for scattered muon triggers, in order to determine the integrated useable flux. In this way hodoscope and reconstruction efficiencies were taken into account. A statistical precision of 1% could be achieved with the second method in a few hours of data taking.

Uncertainties in the incident and scattered muon momenta are important sources of systematic error. The beam momentum measurement system (BMS) was calibrated to an accuracy of $\pm 0.2\%$ at both 90 and 280 GeV, using a purpose built spectrometer [11]. At both energies, the main spectrometer magnet (FSM) was calibrated against the measured masses of the J/ψ and K^0 mesons to an accuracy of $\pm 0.2\%$. The relative calibration of the BMS and FSM for the 280 GeV data was checked in a series of dedicated runs with a system of specially installed silicon microstrip detectors.

During four periods of data taking at 280 GeV, 11.5×10^6 triggers were recorded, whilst at 90 GeV, 5.8×10^6 triggers were taken during one period. The following selections and cuts were applied to the data. The longitudinal position of the reconstructed interaction vertex was required to be within one of the targets. Since beam defining veto hodoscopes had apertures of 3 cm radius, whilst the target cells were 5 cm in radius, the beam was well contained laterally within the target material. To eliminate muons from π and K decays, the scattered muon was required to have a momentum larger than 15 (40) GeV/c in the 90 (280) GeV data set. In order to remove regions of rapidly varying acceptance, minimum scattering angles were imposed of 13 mrad in the upstream and 15 mrad in the downstream targets. Events with ν less than 7 (30) GeV in the 90 (280) GeV data were rejected to ensure good resolution in ν. A requirement of $y < 0.9$ removed kinematic regions where radiative contributions are large. For a given x bin, those Q^2 points whose acceptance was less than 30% of the maximum in that bin were removed.

It was found that some of the large drift chambers used to reconstruct the tracks of the scattered muon suffered inefficiencies due to large event-related background. These chambers (W45, quoted in ref. [6]) were not used in the results presented here because these inefficiencies are not fully understood. The spectrometer's acceptance is then limited by the size of the smaller proportional chambers at the same position (P45, quoted in ref. [7]).

After all cuts there remained 270 000 (131 000) events on hydrogen, and 561 000 (267 000) events on deuterium at 90 (280) GeV. It was checked that imposing more restrictive kinematic cuts did not change the final F_2 values significantly. The kinematic region covered is $0.006 \leqslant x \leqslant 0.6$ and $0.5 \leqslant Q^2 \leqslant 55$ GeV^2. The use of tracks reconstructed in P45 rather than W45 limits the high Q^2 range of each data set; consequently, at present there is no overlap between the results from the two energies.

3. Structure function analysis

An iterative method was employed to extract the structure functions. In this method the spectrometer acceptance was determined with a Monte Carlo simulation; each accepted Monte Carlo event was weighted with the inclusive cross section, i.e. the one-photon exchange cross section together with contributions from radiative and other higher order processes. These weights were computed from an initial

choice of F_2 and a fixed parametrisation of R [12]. A comparison of the normalised yields of data and accepted Monte Carlo events permitted new values of $F_2(x, Q^2)$ to be determined. Parametrisations of the new F_2 values were used to recompute the one photon cross section and the radiative contributions for use in the subsequent iteration. The procedure was repeated until the values of F_2 changed by less than 0.2% – typically after two or three iterations.

The initial F_2 and the form of the parametrisation was that of Appendix A in ref. [8]. In its use here only the 8 parameters describing the deep inelastic region were fitted, while the parametrisation of the resonance region was kept fixed. To check that the results did not depend on the initial values of the parameters, the procedure was repeated starting from a markedly different F_2; using that of calcium arbitrarily multiplied by 0.9 gave structure functions that differed by less than 0.1% after three iterations. The sensitivity of the results to the form of the parametrisation was checked by repeating the procedure using the 15 parameter function of ref. [13]. The differences in the resulting F_2 due to the functional form were negligible everywhere except in the lowest x bin where they were up to 2%. The differences were used point by point as an estimate of this systematic error.

With the present data a determination of R is not possible and it was taken to be that given by the parametrisation of ref. [12], which includes the low x data of CDHSW [14]. The Q^2 behaviour of the parametrisation at low x is consistent with a calculation based on a model due to Nikolaev and Zakharov [15]. To calculate the radiative contributions to the cross section, the parametrisation of R which is valid down to $Q^2=0.35$ GeV^2, has to be extrapolated to lower values of Q^2. We assumed it to be constant with an uncertainty of 100%.

The radiative contributions to the cross section were calculated using the method of Akhundov, Bardin and Shumeiko [16]. This procedure contains the most complete treatment of higher order corrections available. The inputs to the calculation were taken from recent descriptions of available data as discussed in ref. [8]. In the kinematic range of the present measurement the largest radiative contributions to the cross section are less than 35%.

For the proton the calculation of the radiative effects at low x has been checked by Bardin against a calculation developed for HERA [17] and found to be in good agreement. The procedure was compared with that of Mo and Tsai [18] with the inclusion of vacuum polarisation by quark and τ loops and electroweak interference terms. The differences between the results from the two schemes were always less than 2% [19]. The change of radiative correction scheme has a negligible effect on the previously published nucleon structure function ratio [8,20] where the Mo and Tsai approach without the above mentioned terms was used.

In order to determine the systematic error on F_2 due to the inputs to the radiative contribution calculation, the prescription described in ref. [8] was followed. The contributions were recalculated with all inputs moved to the limits of their uncertainties in the direction that maximised the change in the correction and the structure functions redetermined. The dominant contributions to the error are the uncertainty on $R(x, Q^2)$, the parametrisation of the proton form factor and the suppression factor for deuterium. The value of R was changed both in the calculation of the one-photon exchange cross section (eq. (1)) and in the calculation of the radiative contributions. The resulting difference in the structure functions was about 3% (1.5%) for F_2^p (F_2^d) at the lowest x, becoming negligible above $x=0.05$. The difference at each (x, Q^2) point was taken as the contribution to the systematic error.

In the Monte Carlo simulation used to determine the acceptance only the incident and scattered muons (but no hadrons) were tracked, and hits in the detector were generated using parametrisations of the measured efficiencies of the trigger hodoscopes and tracking chambers. A sample of Monte Carlo events equivalent in size to that of the data was generated and passed through the reconstruction programs. In the extraction of the structure functions, differences between data and Monte Carlo are attributed to the difference between the true and assumed structure functions. Therefore, we have checked that the acceptance is well described by the simulation. This was done by comparing distributions of data and Monte Carlo events in variables not, or only weakly, related to x and Q^2, for example the azimuthal angle of the scattered muon. The account for changes in the detector, the acceptance was determined separately for each period of data taking.

Reconstruction losses correlated with multiplicity in the chambers were determined with a further detailed Monte Carlo simulation in which the generation of the complete final state was made. The LUND hadron generator [21] was used to generate the primary hadrons. These were allowed to decay and interact, and the full development of hadronic and electromagnetic showers produced in the apparatus was simulated with the GHEISHA program [22]. The reconstruction inefficiencies were determined by comparing events reconstructed both with and without the inclusion of the simulated backgrounds and were evaluated independently for the 90 an 280 GeV data. No significant difference was observed between the inefficiency for the upstream and the downstream target events, or for hydrogen and deuterium events. The inefficiency was observed to be strongly correlated with the total multiplicity in the chambers. The multiplicities observed in the detectors were well reproduced by the simulation, except for those in the W45 drift chambers. For this reason these chambers were not used in the present analysis. The reconstruction inefficiencies were parametrised as a function of y and the data corrected. The correction was zero for $y<0.2$, rising linearly to 5% (8%) at $y=0.85$ for the 90 (280) GeV data. The small differences observed in the multiplicities between the data and Monte Carlo event samples were used to estimate the uncertainty on the correction. The consequent systematic error on F_2 decreases from 1% (1%) of F_2 at the lowest x for the 90 (280) GeV data, to 0.5% (0.8%) for $x>0.03$.

The accuracy of the acceptance determination was estimated from a comparison of structure functions measured separately in the upstream and downstream targets. They were fitted independently with the 8-parameter functional form described above. The differences between the fits were up to 4% at the lowest x and between 1% and 2% elsewhere. At each (x, Q^2) point half of the difference between the two fit

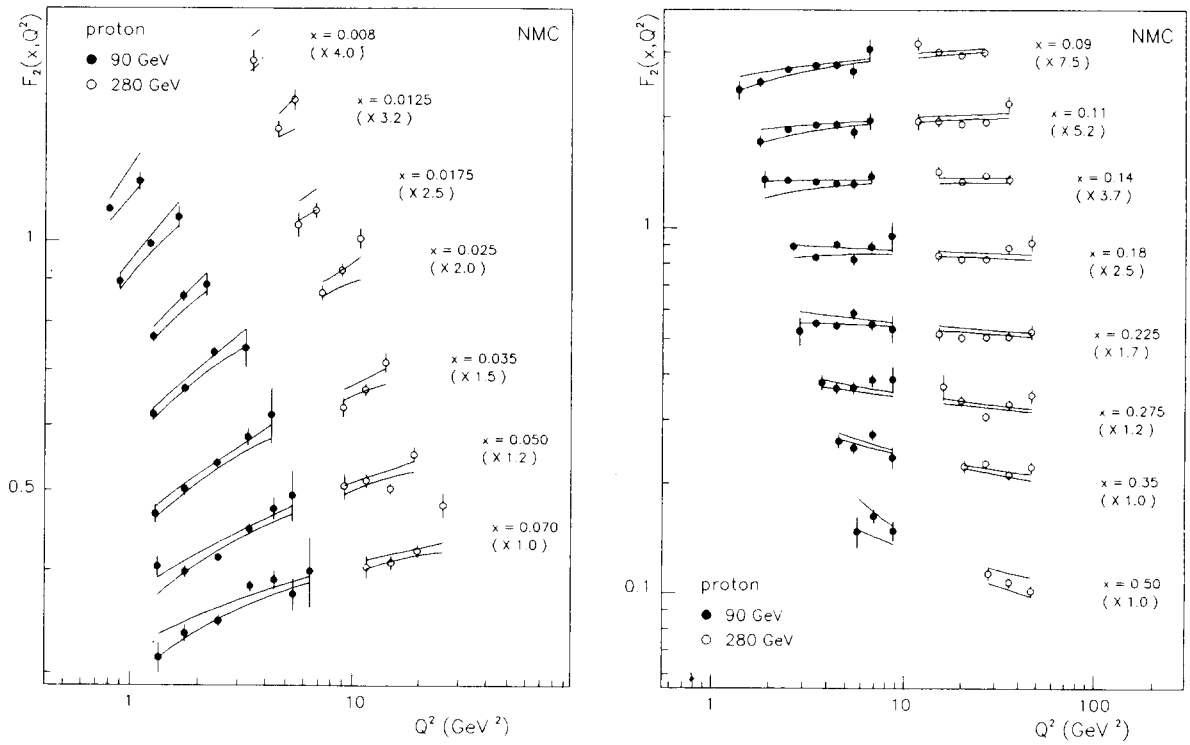

Fig. 1. The proton structure function F_2^p. In the figure the data in each x bin have been scaled by the indicated factor for clarity. The filled symbols represent the 90 GeV data, the open symbols the 280 GeV data. The errors bars represent the statistical errors, the bands the total systematic error excluding the normalisation error of 1.6% (2.6%) of the 90 (280) GeV data.

values was taken as a contribution to the systematic error.

The data from the four 280 GeV periods were found to be consistent, apart from some overall normalisation differences. The structure functions from the individual periods were averaged, and the normalisation spread of $\pm 2\%$ was included in the overall normalisation error. For the single period of 90 GeV, the consistency of the data was checked by splitting the period into five parts. A similar normalisation spread of $\pm 1\%$ was thus estimated. Hence the relative normalisation uncertainty of the 90 GeV with respect to the 280 GeV data is $\pm 2.2\%$. The uncertainty in the relative normalisation of F_2^p with respect to F_2^d is negligible.

The data were normalised to the average of the two measurements of the integrated incident muon flux. These were found to differ by 1.3%, with the random trigger method systematically measuring a smaller flux than the scaler method. This difference does not affect the relative normalisation of the 90 and 280 GeV data sets; half of it was combined with the above normalisation spreads to give total normalisation errors of 1.6% and 2.6% for the 90 and 280 GeV data, respectively.

The data were corrected for a 3.1% contamination of the deuterium with HD molecules. The NMC measurement of F_2^n/F_2^p [8] was used to determine the correction, which varied from 1% at the lowest x, to 0.5% at $x=0.5$, with negligible error. The amount of non-target material within the vertex cuts and the subsequent contamination of the event sample was negligible.

4. Results

The structure functions are shown versus Q^2 for each bin in x in figs. 1 and 2 [#1]. The data clearly ex-

[#1] The values of F_2 and the errors are tabulated in ref. [23].

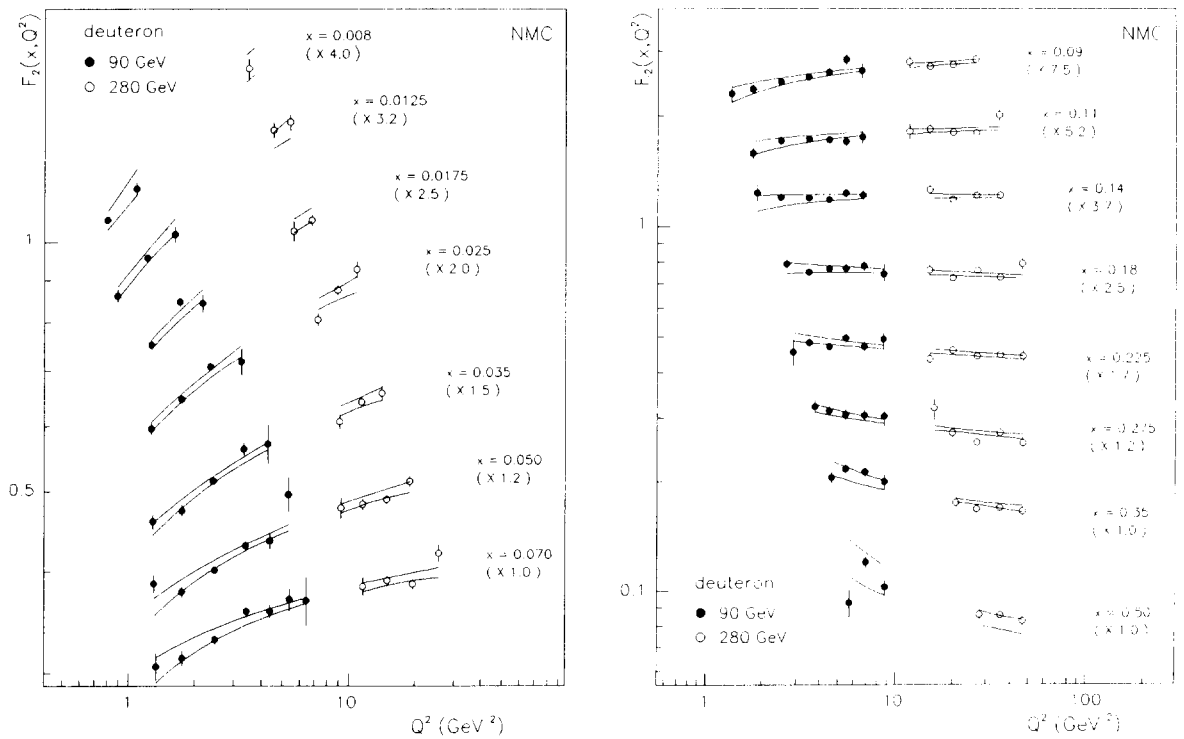

Fig. 2. The deuteron structure function F_2^d. In the figure the data in each x bin have been scaled by the indicated factor for clarity. The filled symbols represent the 90 GeV data, the open symbols the 280 GeV data. The error bars represent the statistical errors, the bands the total systematic error excluding the normalisation error of 1.6% (2.6%) of the 90 (280) GeV data.

hibit the scaling violations expected from perturbative QCD. The slopes, $\mathrm{d}\ln F_2/\mathrm{d}\ln Q^2$, are strongly positive at low x and become negative at larger values of x. In figs. 1 and 2 the error bars represent the statistical errors. The systematic errors due to the radiative corrections, incident and scattered muon energy calibrations, reconstruction inefficiency, functional form of the parametrisation and the acceptance uncertainty were added in quadrature and are shown as the bands. These bands are plotted relative to the function fitted to the data as described above. It should be noted that these errors are correlated between energies and materials, and the reader is referred to ref. [23] for details. The overall normalisation uncertainty is not included in the error bands.

The data used in the present analysis are a subset of those presented in ref. [8] for the measurement of $F_2^n/F_2^p(=2F_2^d/F_2^p-1)$. The ratio F_2^n/F_2^p from the present analysis is consistent with that presented in ref. [8], albeit with larger statistical errors. In the evaluation of the Gottfried sum from the ratio F_2^n/F_2^p [20], we used for F_2^d a fit to the then available world data. If the presently determined F_2^d had been used in that analysis, the value of the Gottfried sum in the measured range would be 0.234 ± 0.008, where the error is statistical only. This is in agreement with the published value. Furthermore, the Gottfried sum obtained directly from F_2^p and F_2^d was found to be consistent with the result given in ref. [20], over the presently measured range.

In figs. 3–5 the deuteron results are compared to those from previous experiments. The error bars shown in these figures are the quadratic sums of the statistical and systematic errors of each experiment, excluding the normalisation errors.

Fig. 3 shows very good agreement between the present data and those of both SLAC [5] and BCDMS [4]. The present data cover part of the Q^2 region of each of the other experiments, and extend to much lower x. The curve plotted in this figure is

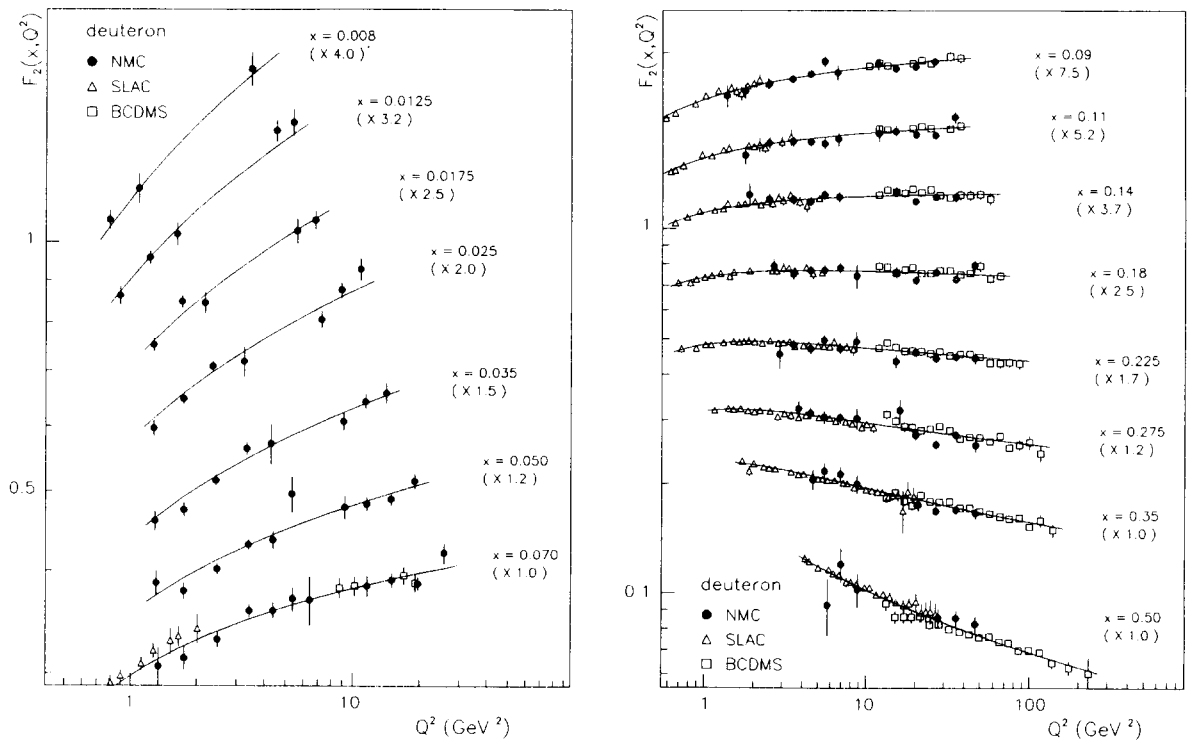

Fig. 3. The present F_2^d (filled symbols) compared with those of SLAC (triangles) and BCDMS (squares). The SLAC and BCDMS data were rebinned to the NMC x bins. The error bars represent the quadratic sum of the statistical and systematic errors. The curve is the result of the fit of the 15-parameter function to all three data sets including data at $x>0.5$ not shown in this figure.

Table 1
The parametrisation of F_2^p, F_2^d. This function is strictly valid only in the kinematic range of the NMC, SLAC and BCDMS data.

$$F_2(x,Q^2)=A(x)\left(\frac{\ln(Q^2/\Lambda^2)}{\ln(Q_0^2/\Lambda^2)}\right)^{B(x)}\left(1+\frac{C(x)}{Q^2}\right),$$

$Q_0^2=20\ \mathrm{GeV}^2$, $\Lambda=250\ \mathrm{MeV}$,

$A(x)=x^{a_1}(1-x)^{a_2}[a_3+a_4(1-x)+a_5(1-x)^2$
$+a_6(1-x)^3+a_7(1-x)^4]$,

$B(x)=b_1+b_2x+b_3/(x+b_4)$,

$C(x)=c_1x+c_2x^2+c_3x^3+c_4x^4$.

Parameter	Proton	Deuteron
a_1	−0.1011	−0.0996
a_2	2.562	2.489
a_3	0.4121	0.4684
a_4	−0.518	−1.924
a_5	5.967	8.159
a_6	−10.197	−10.893
a_7	4.685	4.535
b_1	0.364	0.252
b_2	−2.764	−2.713
b_3	0.0150	0.0254
b_4	0.0186	0.0299
c_1	−1.179	−1.221
c_2	8.24	7.50
c_3	−36.36	−30.49
c_4	47.76	40.23

the result of a fit to the three data sets using the 15-parameter function discussed above (see table 1).

The EMC-NA2 data [2] have recently been re-analysed [24], using the QCD prediction for R in place of the $R=0$ assumed in the original analysis [#2]. These deuteron data are compared with the present results as a function of x for two different values of Q^2 in fig. 4. The SLAC and BCDMS data are also shown for comparison. Systematic differences with EMC of up to 20% at low x are seen. In the light of the studies made of the reconstruction losses in the large drift chambers (W45) it seems likely that the discrepancies at low x are due to such inefficiencies affecting the EMC data.

A comparison with previously published proton

[#2] In this re-analysis by Bazizi and Wimpenny, additional unpublished EMC data were included [25].

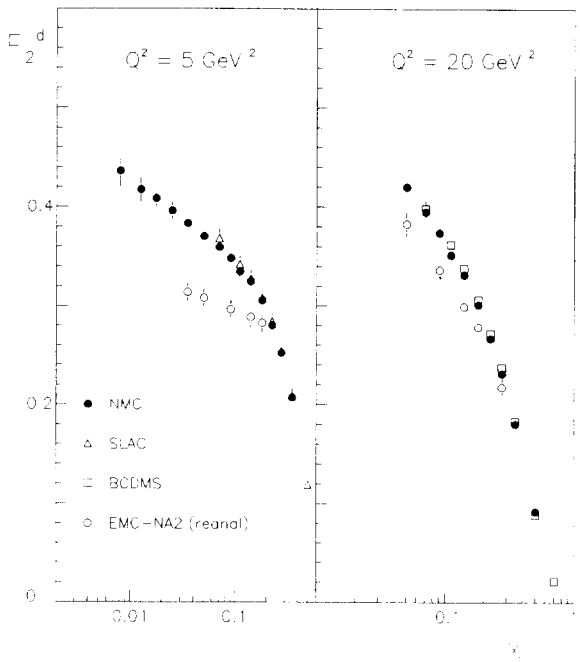

Fig. 4. The present F_2^d compared with those of the re-analysed EMC-NA2 data, and those of SLAC and BCDMS, at a Q^2 of 5 and 20 GeV^2. Only those x points within the measured ranges of each experiment are shown (i.e. with no Q^2 extrapolations). The error bars represent the quadratic sum of the statistical and systematic errors.

data [1,3,5] leads to similar conclusions.

Finally, in fig. 5 the deuteron data are plotted versus x for several bins of Q^2 together with the EMC-NA28 low x measurement [7], and the SLAC data [5]. The EMC-NA28 data are in fair agreement with the present data. Of interest in this figure is the clear x-independence of the structure functions for $Q^2 \lesssim 2.5$ GeV^2 and $x \lesssim 0.1$ as expected from a simple Regge theory.

The low x behaviour of the structure functions (or the parton distributions) is important in determining the reaction rates to be expected in future experiments at higher energies (LHC, SSC). In fig. 6 the present F_2^p is shown compared to those calculated from recent phenomenological parton descriptions, at $Q^2=5$ GeV^2. The curves shown in the figure correspond to the recommended parametrisations (see ref. [26]) of Kwieciński et al. (KMRS-B0) [27], Morfin and Tung (MT-S1) [28]. These parametrisations were constrained by precise data above $x=0.07$

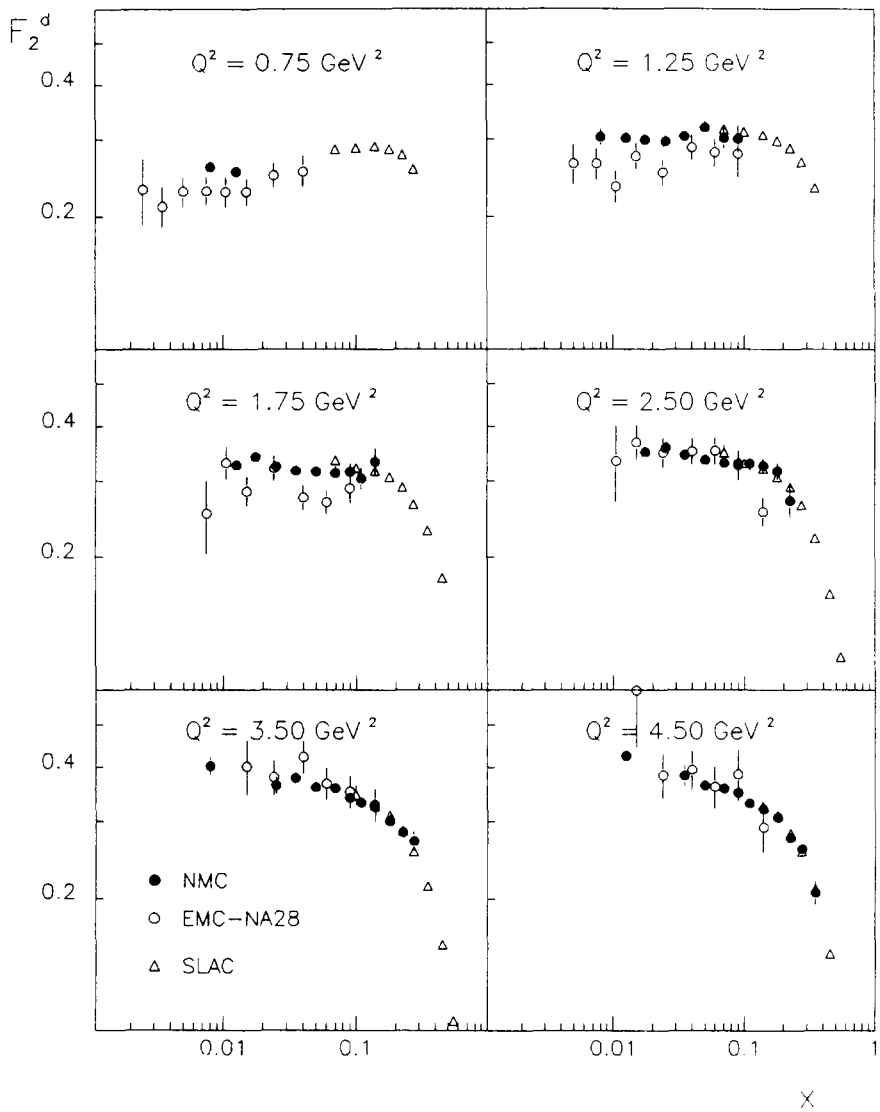

Fig. 5. The present F_2^d compared with those of EMC-NA28 and SLAC as a function of x at several values of Q^2. The error bars represent the quadratic sum of the statistical and systematic errors.

but fail to describe the low x behaviour of the present data. Also shown is the result of a model (in part constrained by experimental data) due to Glück et al. (GRV) [29]. This gives a fair description of the present data.

5. Conclusions

We have presented new measurements of proton and deuteron structure functions over a wide kinematic range: $0.006 \leqslant x \leqslant 0.6$ and $0.5 \leqslant q^2 \leqslant 55$ GeV^2. The data exhibit logarithmic scaling violations down to small values of x, even at low Q^2. In the range of overlap with the previous SLAC and BCDMS data

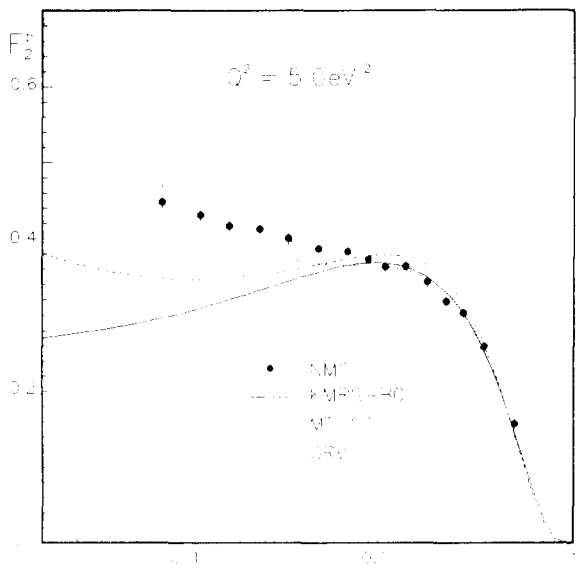

Fig. 6. Recent phenomenological descriptions of F_2^p (KMRS-B0 [27], MT-S1 [28], GRV [29]) compared with the present data.

good agreement is observed between the three experiments. Clear kinematics dependent differences with the EMC-NA2 data are seen. Recent parametrisations of parton distributions fail to describe the x dependence of the structure functions below $x=0.07$. The interpretation of the present data in terms of QCD will follow in a future communication.

Acknowledgement

We would like to thank D.Yu. Bardin for discussion and comparison of the radiative correction procedures, and R. Horisberger for providing the silicon strip detectors.

References

[1] EMC-NA2 Collab., J.J. Aubert et al., Nucl. Phys. B 259 (1985) 189.
[2] EMC-NA2 Collab., J.J. Aubert et al., Nucl. Phys. B 293 (1987) 740.
[3] BCDMS Collab., A.C. Benvenuti et al., Phys. Lett. B 223 (1989) 485.
[4] BCDMS Collab., A.C. Benvenuti et al., Phys. Lett. B 237 (1990) 592.
[5] L. Whitlow et al., Phys. Lett. B 282 (1992) 475.
[6] EMC-NA2 Collab., O.C. Allkofer et al., Nucl. Instrum. Methods 179 (1981) 445.
[7] EMC-NA28 Collab., M. Arneodo et al., Nucl. Phys. B 333 (1990) 1.
[8] NM Collab., P. Amaudruz et al., Nucl. Phys. B 371 (1992) 3.
[9] M. van der Heijden, Ph.D. Thesis, University of Amsterdam (1991);
I.G. Bird, Ph.D. Thesis, Free University (Amsterdam, 1992);
A. Brüll, Ph.D. Thesis, Freiburg University (1992).
[10] R.P. Mount, Nucl. Instrum. Methods 187 (1981) 401.
[11] M. Arneodo, Ph.D. Thesis, Princeton University (1992).
[12] L.W. Whitlow et al., Phys. Lett. B 250 (1990) 193.
[13] A. Milsztajn et al., Z. Phys. C 49 (1991) 527.
[14] CDHSW Collab., P. Berge et al., Z. Phys. C 49 (1991) 187.
[15] N.N. Nikolaev and B.G. Zakharov, Z. Phys. C 49 (1991) 607.
[16] A.A. Akhundov et al., Sov. J. Nucl. Phys. 26 (1977) 660; 44 (1986) 988;
JINR-Dubna preprints E2-10147 (1976), E2-10205 (1976), E2-86-104 (1986);
D. Bardin and N. Shumeiko, Sov. J. Nucl. Phys. 29 (1979) 499.
[17] H. Spiesberger, invited talk at DESY-Zeuthen Workshop on Deep inelastic scattering (April 1992);
D. Bardin, invited talk at DESY-Zeuthen Workshop on Deep inelastic scattering (April 1992).
[18] L.W. Mo and Y.S. Tsai, Rev. Mod. Phys. 41 (1969) 205;
Y.S. Tsai, preprint SLAC-PUB-848 (1971).
[19] B. Badelek, D. Bardin, K. Kurek and C. Scholz, in preparation.
[20] NM Collab., P. Amaudruz et al., Phys. Rev. Lett. 66 (1991) 2712.
[21] The LUND Monte Carlo Programs, CERN pool programs long writeup (April1987), and references therein.
[22] Program GHEISHA, H. Fesefeldt, III. Physikalisches Institut (Aachen), report PITHA 85/02.
[23] NM Collab., P. Amaudruz et al., preprint CERN-PPE/92-124.
[24] K. Bazizi and S.J. Wimpenny, preprint UCR/DIS/91-02.
[25] H. Peschel, Ph.D. Thesis, University of Wuppertal (1990).
[26] H. Plothow-Besch, Parton density functions, Proc. third Workshop on Detector and event simulation in high energy physics (Amsterdam, April 1991);
Program PDFLIB, CERN Program Library Pool W5051 (1991).
[27] J. Kwieciński et al., Phys. Rev. D 42 (1990) 3645.
[28] J.G. Morfin and W.K. Tung, Z. Phys. C 52 (1991) 13.
[29] M. Glück, E. Reya and M. Vogt, Z. Phys. C 53 (1992) 127.